

A Non-Hermitian State-to-State Analysis of Transport in Aggregates with Multiple Endpoints

Devansh Sharma and Amartya Bose^{a)}

Department of Chemical Sciences, Tata Institute of Fundamental Research, Mumbai 400005, India

Efficiency of quantum transport through aggregates with multiple end-points or traps proves to be an emergent and a highly non-equilibrium phenomenon. We present a numerically exact approach for computing the emergent time scale and amount of extraction specific to particular traps leveraging a non-Hermitian generalization of the recently introduced state-to-state transport analysis [Bose and Walters, *J. Chem. Theory Comput.* 2023, **19**, 15, 4828–4836]. This method is able to simultaneously account for the coupling between various sites, the many-body effects brought in by the vibrations and environment held at a non-zero temperature, and the local extraction processes described by non-Hermitian terms in the Hamiltonian. In fact, our non-Hermitian state-to-state analysis goes beyond merely providing an emergent loss time-scale. It can parse the entire dynamics into the constituent internal transport pathways and loss to environment. We demonstrate this method using examples of an exciton transport in a lossy polaritonic cavity. The loss at the cavity and the extraction of the exciton from a terminal molecule provide competing mechanisms that our method helps to unravel, revealing extremely interesting non-intuitive physics. This non-Hermitian state-to-state analysis technique contributes an important link in understanding and elucidating the routes of transport in open quantum systems.

Various molecular aggregates function as wires, transferring charges and excitation from one end to the other. A prime example of such transport happening in nature are the so-called light-harvesting antenna complexes that absorb solar photons converting them into excitons, which are then shuttled to the reaction center where further reactions take place. These natural systems often have unprecedented efficiencies, which have been a subject of extensive study.^{1–4} It is important to be able to quantify and simulate the efficiency of transport in these complex aggregates. The thermal environment modulates these transfers in a non-perturbative manner. Consequently, advanced wave function-based techniques like the density matrix renormalization group (DMRG)^{5–7} or the multi-configuration time-dependent Hartree (MCTDH)^{8,9} cannot be used effectively since they are incapable of capturing the continuum manifold of environmental states that are thermally accessible.

Simulations involving reduced density matrix provide a lucrative approach to understanding such non-equilibrium transport. Heijs *et al.*¹⁰ and Cao & Silbey¹¹ have explored the relation between trapping time and efficiency, providing a classical kinetic picture. Efficiency of quantum transport has been studied using approximate^{12,13} and numerically exact methods.¹⁴ Sener *et al.*¹⁵ and others have explored the robustness of photosynthetic transport. Approximate methods are often plagued by *ad hoc* assumptions that may fail for a particular system. In this context, numerically exact simulations using methods like hierarchical equations of motion (HEOM)^{16–20} or the quasi-adiabatic propagator path integral (QuAPI)^{21–27} are extremely useful. They however require a full description of the end-point from which the

extraction happens, the sites to which the extraction happens, and their thermal environments to be able to predict the efficiency of the transport. Many transport aggregates may even have more than one end-point or trap site. In such cases, this already challenging parameterization requirement is followed by an exponential growth of complexity due to a growth of the system Hilbert space with every extra trap site. Additionally, many processes like spontaneous emission from an excited state, or loss from a leaky cavity in case of a polaritonic system cannot be simply expressed as a well-characterized harmonic bath. These processes are naturally defined in terms of empirical time-scales. The grand challenge, therefore, is simulating the dynamics under empirical loss processes using numerically exact methods and then calculating the individual efficiencies of the different traps in a multi-trap transport process.

The recently developed path integral Lindblad dynamics framework (PILD)²⁸ allows for a combination of Lindblad master equation to incorporate the loss or gain processes and numerically rigorous path integrals to account for the effects of the thermal environment. PILD has been used to study the effect of loss processes on exciton transport dynamics in Fenna-Matthews-Olson complex²⁸ as well as on linear spectra of chiral aggregates.²⁹ In many cases, the use of non-Hermitian descriptions of the system coupled with path integrals to incorporate the dissipative environment provides an alternative route to study the dynamics.³⁰ While the non-unitarity of the propagators make it inherently unsuited for spectra represented by correlation functions that couple the ground and the excited state manifolds, it can be enough for the study of dynamics.

Understanding the time-scale of transport in aggregates with multiple monomers, while important, turns out to be quite challenging. Imagine an aggregate where,

^{a)} Electronic mail: amartya.bose@tifr.res.in

in the simplest case, the exciton or other quantum particle is extracted from one of the molecular sites, called the “trap” site, with a “local” time-scale of T time units. This T units, which is the time-scale of extraction from an isolated site, is not the time-scale which one would actually observe in the aggregate. From the site of exciton injection, it would have traveled to all accessible sites and the fraction that is on the trap site would get extracted. This combination of non-equilibrium processes gives rise to an emergent time-scale τ for the extraction as observed, when a particular site is initially excited. It is this emergent time-scale, τ , that is of interest to us. The problem becomes even more challenging when there are multiple trap sites with different local extraction time-scales, T_j , splitting the single exciton in different proportions. A relevant example of this multi-trap transport turns out to be a single channel transport aggregate coupled to a lossy Fabry-Pérot cavity — the loss at the cavity providing a different trapping channel which, while useless to the transport, needs to be incorporated. The question then becomes one of assigning a site-specific emergent time-scale τ_j and also understanding how much of the exciton is extracted (L_j^∞) from each such site.

In this work, we address this question of calculating the trap-specific transport efficiency corresponding to a multi-trap transport aggregate in terms of the emergent site-specific timescale, τ_j , and exciton extraction, L_j^∞ , by generalizing the recently derived state-to-state analysis³¹ for Hamiltonians with on-site non-Hermiticities, describing the rates of leakage from the different traps. This allows us to partition the total leakage of the system into the different sites enabling us to build an intuitive picture for the efficiency of transport for a particular non-equilibrium initial condition without any *ad hoc* approximations.

Consider the following Hamiltonian that describes an open quantum system:

$$\hat{H} = \hat{H}_0 + \hat{H}_{\text{env}} \quad (1)$$

where \hat{H}_0 describes the system and \hat{H}_{env} describes the environment and its interaction with the system. For concreteness, let us assume that the system is described by a Frenkel Hamiltonian where each of the basis vectors $|j\rangle$ represents the quantum particle (charge or excitation) is on the j th site or molecule and every other site being empty. The system, then, is generically described by the non-Hermitian operator,

$$\hat{H}_0 = \sum_j \epsilon_j |j\rangle\langle j| + \sum_{j < k} h_{jk} (|j\rangle\langle k| + |k\rangle\langle j|), \quad (2)$$

where $h_{jk} \in \mathbb{R}$ is the coupling or hopping parameter between the j th and the k th sites, and $\epsilon_j \in \mathbb{C}$ is the energy of the system when the particle is on the j th site with the corresponding lifetime. The real part of ϵ_j represents the site energy while the imaginary part of ϵ_j , wherever non-zero, represents the rate of loss from the

j th site corresponding to the “local” decay time T_j with $\text{Im}(\epsilon_j) = -\pi\hbar/T_j$.

Some or all of the sites are individually coupled to thermal environments

$$\hat{H}_{\text{env}} = \sum_j \hat{H}_{\text{env}}^{(j)} \quad (3)$$

$$\hat{H}_{\text{env}}^{(j)} = \sum_b \frac{p_{jb}^2}{2} + \frac{1}{2}\omega_{jb}^2 x_{jb}^2 - c_{jb} x_{jb} \hat{s}_j \quad (4)$$

where the bath on the j th site is coupled to the system through the system operator \hat{s}_j . Each bath of harmonic oscillators is characterized by the oscillators’ frequencies ω_{jb} and their corresponding couplings c_{jb} . These are related to the spectral density,

$$J_j(\omega) = \frac{\pi}{2} \sum_b \frac{c_{jb}^2}{\omega_{jb}} \delta(\omega - \omega_{jb}), \quad (5)$$

which can be estimated using molecular dynamics simulations^{32,33} or directly from experiments.

After an initial Frank-Condon excitation of a molecule in the aggregate, the state of the system can be written in a separable form $\rho(0) = \tilde{\rho}(0) \otimes e^{-\beta H_{\text{env}}}/Z$. The time-evolved reduced density matrix can be written in terms of path integrals^{21,22} (augmented for non-Hermitian systems³⁰) as,

$$\begin{aligned} \langle s_N^+ | \tilde{\rho}(N\Delta t) | s_N^- \rangle &= \sum_{s_j^\pm} \langle s_N^+ | U | s_{N-1}^+ \rangle \langle s_{N-1}^+ | U | s_{N-2}^+ \rangle \cdots \\ &\quad \times \langle s_1^+ | U | s_0^+ \rangle \langle s_0^+ | \rho(0) | s_0^- \rangle \langle s_0^- | \bar{U} | s_1^- \rangle \\ &\quad \times \cdots \langle s_{N-1}^- | \bar{U} | s_N^- \rangle \times F[\{s_j^\pm\}] \quad (6) \end{aligned}$$

where $U = \exp(-i\hat{H}_0\Delta t/\hbar)$ is the forward propagator, and $\bar{U} = \exp(i\hat{H}_0^\dagger\Delta t/\hbar)$ is the backward propagator. Notice that the non-Hermiticity of the system ($\hat{H}_0 \neq \hat{H}_0^\dagger$) is taken into account in the definition of the backward propagator. In the path integral, the state of the system at the j th time point is s_j^\pm . The Feynman-Vernon influence functional,³⁴ $F[\{s_j^\pm\}]$, captures the system-environment interaction and makes the dynamics non-Markovian. It is dependent upon the spectral density.³³ In a condensed phase medium, the decay of the memory with time allows for a truncation of the memory and iteration beyond this memory length. However, the cost of simulation still increases exponentially within the memory length. Here, we use the time-evolving matrix product operator (TEMPO) algorithm²⁴ adapted for non-Hermitian systems to do the simulations efficiently. This is implemented in the recently released `QuantumDynamics.jl` package.³⁵

Now, because of the non-Hermiticity of \hat{H}_0 and the consequent non-unitarity of the time-evolution, $\text{Tr}[\tilde{\rho}(t)] \leq 1$. In fact, the trace is a monotonically decreasing quantity and for the single excitation subspace,

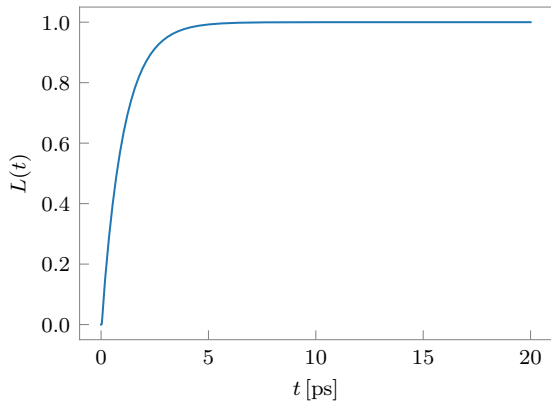


FIG. 1. Excitation loss $L(t)$ in the excitonic trimer with a single trap starting with an initial excitation $\tilde{\rho}(0) = |1\rangle\langle 1|$ and $T_3 = 0.3$ ps.

the quantity $L(t) = 1 - \text{Tr}[\tilde{\rho}(t)]$ is the amount of excitation that has leaked out of the system. As a simple example, consider excitation transport in an excitonic trimer of identical monomers, with a constant nearest-neighbor electronic coupling $h_{jk} = h = -181.5 \text{ cm}^{-1} \delta_{k,j+1}$ and an exciton drain on the third monomer with a decay time of $T_3 = 0.3$ ps. This coupling is representative of typical electronic couplings in bacteriochlorophyll chains.^{36–38} The vibronic couplings and the solvent interactions associated with each monomer is modeled as

$$J(\omega) = \frac{\pi}{2} \hbar \xi \omega \exp(-\omega/\omega_c), \quad (7)$$

where $\xi = 0.121$ and $\omega_c = 900 \text{ cm}^{-1}$ corresponding to a reorganization energy $\lambda_0 = 218 \text{ cm}^{-1}$. The temperature is set to 300 K. (This particular system will be used in different contexts throughout the paper. For simplicity, we will refer to it as the “excitonic trimer.”) The transport starts with excitation on the first monomer, $\tilde{\rho}(0) = |1\rangle\langle 1|$. The loss $L(t)$ for the excitonic trimer is shown in Figure 1. The emergent time-scale of loss, obtained with the model fit $L(t) = 1 - \exp(-t/\tau)$, is $\tau = 1.04$ ps, which is significantly longer than the local loss time-scale of $T_3 = 0.3$ ps.

If we were interested in the transport through a system with only one trap site, then considering the dynamics of $L(t)$ as demonstrated would be adequate. However, we want to generalize this to molecular aggregates with multiple traps, where we would like to extract the trap-specific efficiency. The primary complication that arises with the previous argument of the loss being the change in the trace of the density matrix applied to this case is that the loss can now happen through more than one site. How do we figure out the partitioning of this total loss into the constituent single site losses? To achieve this, we generalize the concept of the state-to-state transfer³¹ to account for non-Hermitian systems.

Consider the rate of change of population of the j th

site,

$$\frac{\partial P_j}{\partial t} = \frac{\partial}{\partial t} \text{Tr}_{\text{sys-env}} [\rho(t) |j\rangle\langle j|], \quad (8)$$

where $\rho(t)$ is the time-evolved density matrix in the full system-environment Hilbert space. Because the Hamiltonian is non-Hermitian, one can write the quantum Liouville equation as

$$\frac{\partial \rho}{\partial t} = -\frac{i}{\hbar} (\hat{H}\rho - \rho\hat{H}^\dagger). \quad (9)$$

Consequently, Eq. 8 can be written as

$$\frac{\partial P_j}{\partial t} = -\frac{i}{\hbar} \text{Tr}_{\text{sys-env}} \left[(\hat{H}\rho - \rho\hat{H}^\dagger) |j\rangle\langle j| \right] \quad (10)$$

$$= \frac{i}{\hbar} \text{Tr}_{\text{sys}} \left[\tilde{\rho}(t) (\hat{H}_0^\dagger |j\rangle\langle j| - |j\rangle\langle j| \hat{H}_0) \right], \quad (11)$$

using the fact that the projector, $|j\rangle\langle j|$, commutes with \hat{H}_{env} . Expanding the trace, we can now partition this flux into the source sites:

$$\begin{aligned} \frac{\partial P_j}{\partial t} = \frac{i}{\hbar} \sum_k \left(\langle j|\tilde{\rho}(t)|k\rangle \langle k|\hat{H}_0^\dagger|j\rangle \right. \\ \left. - \langle j|\hat{H}_0|k\rangle \langle k|\tilde{\rho}(t)|j\rangle \right) \end{aligned} \quad (12)$$

For every k , the summand expresses the instantaneous rate of transfer from k to j and the total rate of change of the population of the j th site is given as a sum over all k as expressed in Eq. 12. Integrating over time, one gets the total partitioned transfer between the k th and the j th sites till time t :

$$\begin{aligned} P_{j\leftarrow k}(t) = \frac{i}{\hbar} \int_0^t dt' \left(\langle k|\hat{H}_0^\dagger|j\rangle - \langle j|\hat{H}_0|k\rangle \right) \text{Re} \langle j|\tilde{\rho}(t')|k\rangle \\ - \frac{1}{\hbar} \int_0^t dt' \left(\langle k|\hat{H}_0^\dagger|j\rangle + \langle j|\hat{H}_0|k\rangle \right) \text{Im} \langle j|\tilde{\rho}(t')|k\rangle \end{aligned} \quad (13)$$

This equation is completely general. For Hermitian systems, only the second term survives, and the expression reduces to the previously derived expression for state-to-state transport.^{31,39} The extra physics corresponding to the losses are all incorporated in the first term. Because non-Hermiticity is limited to the diagonal on-site terms, note that the site-to-site transport ($j \neq k$) is still governed only by the second term, which becomes $P_{j\leftarrow k}(t) = -\frac{2}{\hbar} \int_0^t dt' \langle j|\hat{H}_0|k\rangle \text{Im} \langle j|\tilde{\rho}(t')|k\rangle$. For the self transfer terms ($j = k$), the second term becomes zero because the diagonal elements of the density matrix are real. However the first term is non-zero with $P_{j\leftarrow j}(t) = \frac{2}{\hbar} \int_0^t dt' \text{Im} \langle j|\hat{H}_0|j\rangle \text{Re} \langle j|\tilde{\rho}(t')|j\rangle$. Notice that if a site has a loss term, $\text{Im} \langle j|\hat{H}_0|j\rangle < 0$ and $P_{j\leftarrow j}(t) < 0$ symbolizing a loss from the site into the environment. Thus, the loss through the j th site, $L_j(t)$, is identified with $P_{j\leftarrow j}(t)$, and the total loss can be expressed as a

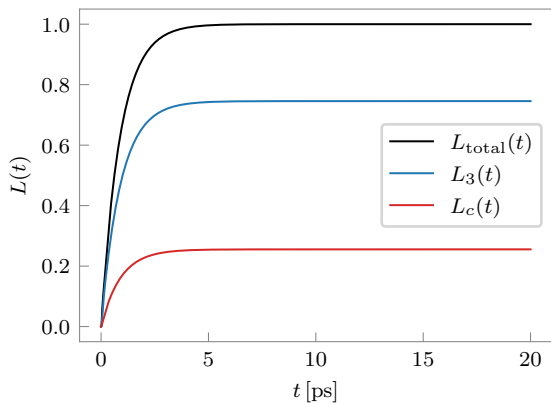


FIG. 2. Excitation loss $L(t)$ in the polaritonic trimer starting with an initial excitation $\tilde{\rho}(0) = |1\rangle\langle 1|$ through an exciton drain of decay time $T_3 = 0.3$ ps coupled to a leaky optical cavity of lifetime $T_c = 0.6$ ps.

sum over all the site-based losses. To obtain the emergent time-scale, this can now be fit to the following model (assuming a single exponential decay),

$$L_j(t) = L_j^\infty (1 - \exp(-t/\tau_j)) \quad (14)$$

where τ_j is the emergent decay time for site j and L_j^∞ is the net loss through that site. These quantities will now be used to characterize efficiency of transport with a single time-scale. Notice that $L_j(0) = 0$ and $\lim_{t \rightarrow \infty} L_j(t) = L_j^\infty$.

In order to demonstrate this method, we consider a polaritonic system — the same excitonic trimer of identical monomers as discussed earlier now coupled to a leaky Fabry-Pérot cavity of energy $\hbar\omega_c$ with a coupling strength of $\Omega = 181.5 \text{ cm}^{-1}$. The cavity mode energy is set in resonance with the monomer’s vertical (Frank-Condon) excitation energy. The new system Hamiltonian \hat{H}'_0 is given by

$$\hat{H}'_0 = \hat{H}_0 + \hbar(\omega_c - i\pi/T_c) |c\rangle\langle c| + \sum_j \Omega (|j\rangle\langle c| + |c\rangle\langle j|), \quad (15)$$

where $|c\rangle$ is the cavity mode. The cavity mode has a lifetime T_c of 0.6 ps, which is slightly on the longer side.⁴⁰ Note that the cavity is not associated with any bath. (This system will be called the “polaritonic trimer.”) The initial excitation is again set to be on the first monomer, $\tilde{\rho}(0) = |1\rangle\langle 1|$. The loss from the third monomer (exciton drain) and the cavity are shown in Figure 2. As mentioned, the total loss, $L(t)$, is the sum of losses from the exciton drain, $L_3(t)$, and the cavity, $L_c(t)$. The emergent loss time-scales for the exciton drain, τ_3 , and cavity, τ_c , are 0.89 ps and 0.90 ps, respectively. In this case, a large majority (around 74%) of the extraction happens through the molecular drain site.

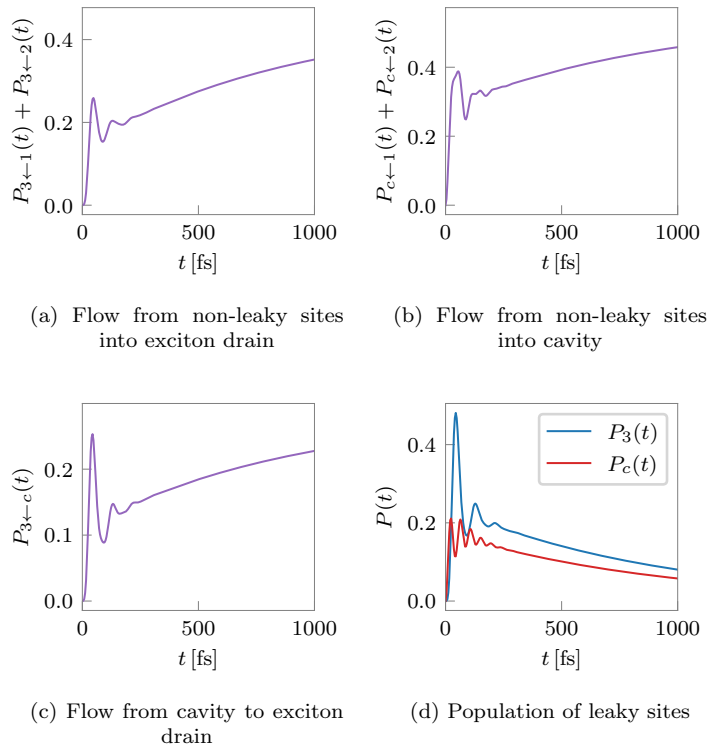


FIG. 3. A state-to-state analysis of excitation flows into the trap sites and their population dynamics for the polaritonic trimer.

It is pertinent at this point to ask how exactly is the excitation flowing through the system to reach these leaky sites. A state-to-state analysis is presented in Figure 3 to show the excitation flows to the leaky sites along with their populations. Notice that at very short times, the flow from the non-leaky sites, $|1\rangle$ and $|2\rangle$, into the cavity $|c\rangle$ (Figure 3 (b)) is more than that into the exciton drain site $|3\rangle$ (Figure 3 (a)). This is because both $|1\rangle$ and $|2\rangle$ transfer population to the cavity site, whereas only $|2\rangle$ transfers to $|3\rangle$ owing to the nearest-neighbor nature of the excitonic Hamiltonian. However, very soon the transfer from $|2\rangle$ to $|3\rangle$ catches up. What is very interesting is that there is a non-insignificant flow from the cavity site $|c\rangle$ to the exciton drain site $|3\rangle$ from very early times (Figure 3 (c)). All of this along with the leakages from $|c\rangle$ and $|3\rangle$ come together to give the total population dynamics that we can see in Figure 3 (d). Notice that the initial build up of population is higher in $|3\rangle$ than in the cavity even though the leakage on the cavity in this case is slower than that of the monomer.

Now let us see what happens when the reorganization energy of the monomeric environment increases. The losses through the exciton drain $L_3(t)$ for the same system Hamiltonian parameters but with different bath reorganization energies are presented in Figure 4. It is clear that the amount of extraction through the third monomer (L_3^∞) increases with the reorganization energy.

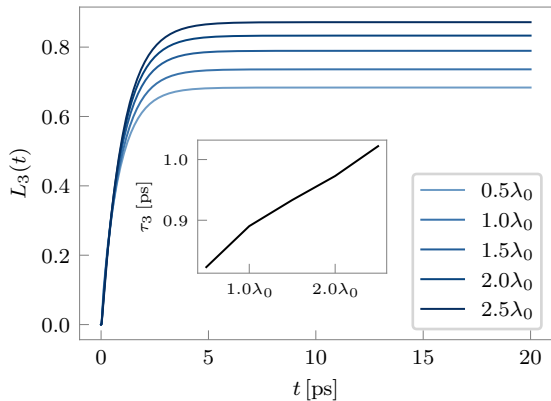


FIG. 4. Loss through exciton drain $L_3(t)$ with increasing bath reorganization energies, λ , and the emergent time-scales τ_3 (inset) for the polaritonic trimer.

As a corollary, this would imply that the amount of leakage through the cavity is decreasing. To understand this better, recall that the cavity energy is set to be resonant with the Frank-Condon (vertical) excitation energy of the monomer. The higher the reorganization energy, the greater is the shift between the ground and excited states of the monomer because the reorganization energy per “mode” is proportional to the Huang-Rhys factor and consequently the relative displacement of the surfaces. In Figure 5, a schematic is shown for the current situation. Suppose that $|e\rangle$ is the excited state surface for the lower reorganization energy environment and $|e'\rangle$ is the one for the higher reorganization energy environment. Notice that $d' > d$. Now, to ensure that the vertical excitation energy remains constant, the surface of $|e'\rangle$ has to be stabilized more. This means that the minimum of the excited state potential energy surface gets increasingly detuned from the cavity energy, hampering the transport into the cavity mode from the monomers. In Figure 6, we show the population of the cavity site. Notice that the accumulation of excitation in the cavity mode decreases with increasing reorganization energy on the monomers. This verifies the argument presented.

Having discussed the increase in L_3^∞ as a function of λ , we turn our attention to the emergent time-scales. From the inset plot in Figure 4, we see that τ_3 increases monotonically with λ . The initial slopes of the loss curves in Figure 4 are identical. This coupled with the fact that the L_3^∞ values are increasing with the reorganization energy, means that the time-scale of exciton leakage through the third monomer, τ_3 , also increases. This becomes obvious if we remember that according to Equation 14, τ_j is effectively related to the half-life of the particle leaking out of the j th monomer.

It should be noted here that it is not necessary that the loss dynamics would have a single time-scale. In fact, the exponential fit to the loss function, Equation 14, begins to fail when the reorganization energy of the environ-

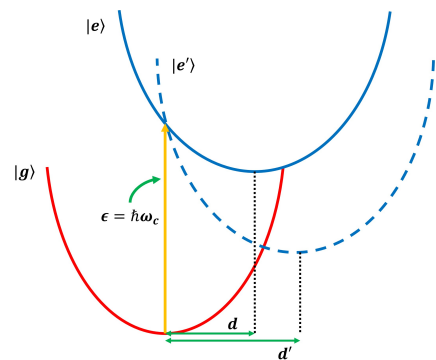


FIG. 5. Schematic depicting shift in excited energy surfaces for two baths differing in their reorganization energies. The $|e'\rangle$ surface corresponds to the higher reorganization energy bath than the $|e\rangle$ surface leading to larger displacement $d' > d$.

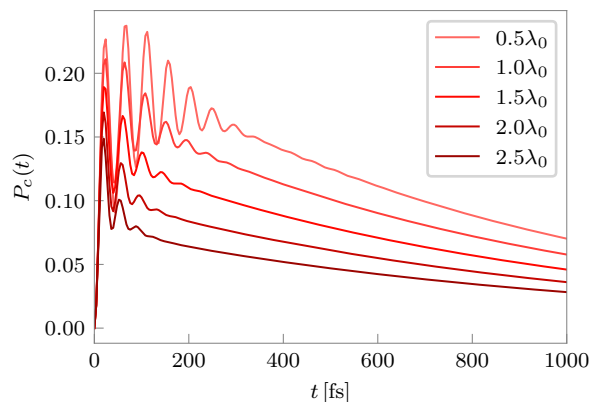


FIG. 6. Population of the cavity site, $P_c(t)$, for different reorganization energies, λ , in the polaritonic trimer.

ment decreases beyond a certain limit due to a preponderance of transients in the dynamics. This parallels failure of rate theory to predict the actual dynamics when transients are important.⁴¹ The present non-Hermitian state-to-state analysis method can be used even when this happens. It is just that we would not be able to talk in terms of the emergent time-scales and would have to directly study the loss curves similar to the ones in Figure 4.

As a final bit of exploration, let us see how the transport efficiency of exciton drain gets affected vis-à-vis the change in cavity properties — monomer-cavity coupling, Ω , and cavity leakage rate, $\gamma_c (= 1/T_c)$. It is more meaningful to vary these parameters relative to their monomeric counterparts — h and $\gamma_3 (= 1/T_3)$. Figure 7 (a) and (b) show the change of L_3^∞ and τ_3 respectively as functions of γ_c/γ_3 for different cavity couplings Ω/h keeping the environment at a constant reorganization energy of λ_0 . First consider the amount of excitation extracted from the third monomer, L_3^∞ , shown in Figure 7 (a). As a function of γ_c/γ_3 it goes down monotonically.

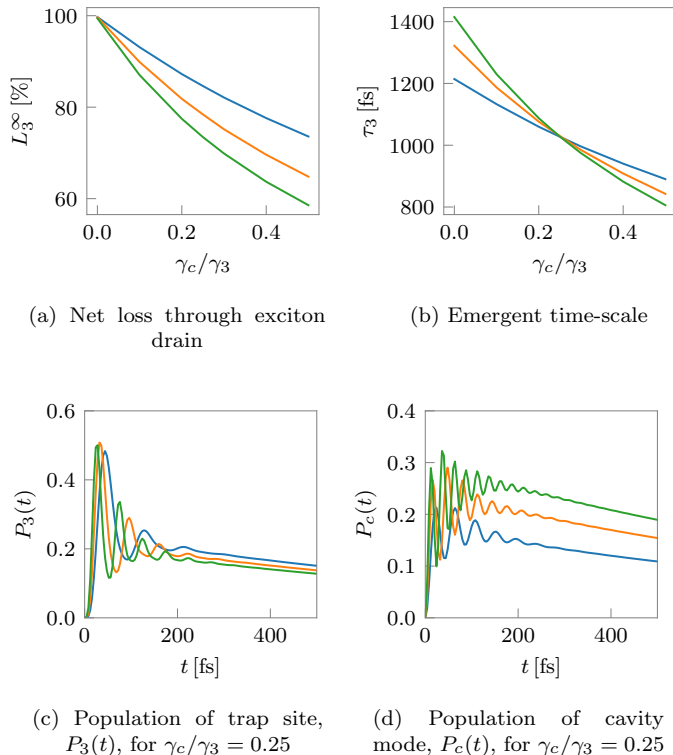


FIG. 7. Analysis of loss mechanisms in the polaritonic aggregate on changing relative loss rates and couplings.

cally because for the same Ω/h , when γ_c increases relative to γ_3 , then more loss happens out of the cavity. What is interesting is that for a particular γ_c/γ_3 , the value of L_3^∞ decreases on increasing Ω/h . To understand this better, we plot the excitonic population of the third monomer and the cavity as a function of time for the three values of Ω/h at a constant $\gamma_c/\gamma_3 = 0.25$ in Figure 7 (c) and (d) respectively. Notice that as Ω/h increases, the amount of population buildup on the cavity increases, but the accumulation on the third monomer decreases. This correspondingly means that there is comparatively less population to be extracted out of $|3\rangle$, leading to a decrease in L_3^∞ .

In Figure 7 (b), we see that the τ_3 values for a constant Ω/h decrease monotonically with γ_c/γ_3 as well. Probably this is related to having less amount of exciton extracted from the molecular drain (L_3^∞). We conclude our discussion of this particular problem by pointing out a surprising observation for future exploration: the τ_3 curves for different Ω/h in Figure 7 (b) all intersect at a point. This raises several very interesting questions: Why do we have this point of intersection? Do polaritonic aggregates of different sizes all have similar points of intersection? How does it change with changing bath on each site? These interesting problems will be dealt with in a future publication using the non-Hermitian state-to-state analysis technique developed in the current letter.

In conclusion, we have described a new way for analyz-

ing the end-point or trap specific efficiency of a multi-trap transport aggregate described by a non-Hermitian Hamiltonian. This method is numerically exact when paired with exact dynamics and makes no additional approximations. While here we have explored the time-scales of transport, there can be several cases, where the extraction process may not be appropriately described by a curve with a single time scale. For such cases, the current non-Hermitian state-to-state analysis technique can yield the full dynamics of extraction. In addition, being a generalization of the state-to-state analysis technique,³¹ this method also allows us to explore the exact pathways of transport under these leakages. In the examples shown, we demonstrated how the non-Hermitian state-to-state method can be used to understand transport in a polaritonic aggregate, where the exciton is extracted from one of the molecules and the cavity is lossy. Of course, in such a case, any loss of the excitation as a photon through the cavity does not count towards transport. Using our non-Hermitian state-to-state method, we are able to partition the total loss into the loss through the cavity and that through the molecule. In the process, we reveal a wealth of extremely rich physics. While the examples showed here used exact dynamics generated using path integrals, one could as well use approximate semiclassical or perturbative methods to generate the dynamics. This method promises to be an extremely powerful analysis tool for understanding the dynamics of complex systems.

¹G. S. Engel, T. R. Calhoun, E. L. Read, T.-K. Ahn, T. Mančal, Y.-C. Cheng, R. E. Blankenship, and G. R. Fleming, “Evidence for wavelike energy transfer through quantum coherence in photosynthetic systems,” *Nature* **446**, 782–786 (2007).

²A. Ishizaki and G. R. Fleming, “Theoretical examination of quantum coherence in a photosynthetic system at physiological temperature,” *Proceedings of the National Academy of Sciences* **106**, 17255–17260 (2009).

³H.-G. Duan, V. I. Prokhorenko, R. J. Cogdell, K. Ashraf, A. L. Stevens, M. Thorwart, and R. J. D. Miller, “Nature does not rely on long-lived electronic quantum coherence for photosynthetic energy transfer,” *Proceedings of the National Academy of Sciences* **114**, 8493 (2017).

⁴H.-G. Duan, A. Jha, L. Chen, V. Tiwari, R. J. Cogdell, K. Ashraf, V. I. Prokhorenko, M. Thorwart, and R. J. D. Miller, “Quantum coherent energy transport in the Fenna–Matthews–Olson complex at low temperature,” *Proceedings of the National Academy of Sciences* **119**, e2212630119 (2022).

⁵S. R. White, “Density matrix formulation for quantum renormalization groups,” *Physical Review Letters* **69**, 2863–2866 (1992).

⁶U. Schollwöck, “The density-matrix renormalization group,” *Reviews of Modern Physics* **77**, 259–315 (2005).

⁷U. Schollwöck, “The density-matrix renormalization group in the age of matrix product states,” *Annals of Physics* **326**, 96–192 (2011).

⁸H.-D. Meyer, U. Manthe, and L. Cederbaum, “The multi-configurational time-dependent Hartree approach,” *Chemical Physics Letters* **165**, 73–78 (1990).

⁹M. Beck, A. Jäckle, G. A. Worth, and H.-D. Meyer, “The multiconfiguration time-dependent Hartree (MCTDH) method: A highly efficient algorithm for propagating wavepackets,” *Physics Reports* **324**, 1–105 (2000).

¹⁰D.-J. Heijs, V. A. Malyshev, and J. Knoester, “Trapping time statistics and efficiency of transport of optical excitations in dendrimers,” *The Journal of Chemical Physics* **121**, 4884–4892 (2004).

- ¹¹J. Cao and R. J. Silbey, "Optimization of Exciton Trapping in Energy Transfer Processes," *The Journal of Physical Chemistry A* **113**, 13825–13838 (2009).
- ¹²C. Uchiyama, W. J. Munro, and K. Nemoto, "Environmental engineering for quantum energy transport," *npj Quantum Information* **4**, 33 (2018).
- ¹³A. G. Dijkstra and A. Beige, "Efficient long-distance energy transport in molecular systems through adiabatic passage," *The Journal of Chemical Physics* **151**, 034114 (2019).
- ¹⁴C. Kreisbeck, T. Kramer, M. Rodríguez, and B. Hein, "High-Performance Solution of Hierarchical Equations of Motion for Studying Energy Transfer in Light-Harvesting Complexes," *Journal of Chemical Theory and Computation* **7**, 2166–2174 (2011).
- ¹⁵M. K. Sener, D. Lu, T. Ritz, S. Park, P. Fromme, and K. Schulten, "Robustness and Optimality of Light Harvesting in Cyanobacterial Photosystem I," *The Journal of Physical Chemistry B* **106**, 7948–7960 (2002).
- ¹⁶Y. Tanimura and R. Kubo, "Time Evolution of a Quantum System in Contact with a Nearly Gaussian-Markoffian Noise Bath," *Journal of the Physical Society of Japan* **58**, 101–114 (1989).
- ¹⁷Y. Tanimura, "Reduced hierarchical equations of motion in real and imaginary time: Correlated initial states and thermodynamic quantities," *The Journal of Chemical Physics* **141**, 044114 (2014), <https://doi.org/10.1063/1.4890441>.
- ¹⁸Y. Tanimura, "Numerically "exact" approach to open quantum dynamics: The hierarchical equations of motion (HEOM)," *The Journal of Chemical Physics* **153**, 20901 (2020).
- ¹⁹M. Xu, Y. Yan, Q. Shi, J. Ankerhold, and J. T. Stockburger, "Taming Quantum Noise for Efficient Low Temperature Simulations of Open Quantum Systems," *Physical Review Letters* **129**, 230601 (2022).
- ²⁰T. Ikeda and G. D. Scholes, "Generalization of the hierarchical equations of motion theory for efficient calculations with arbitrary correlation functions," *The Journal of Chemical Physics* **152**, 204101 (2020).
- ²¹N. Makri and D. E. Makarov, "Tensor propagator for iterative quantum time evolution of reduced density matrices. I. Theory," *The Journal of Chemical Physics* **102**, 4600–4610 (1995).
- ²²N. Makri and D. E. Makarov, "Tensor propagator for iterative quantum time evolution of reduced density matrices. II. Numerical methodology," *The Journal of Chemical Physics* **102**, 4611–4618 (1995).
- ²³N. Makri, E. Sim, D. E. Makarov, and M. Topaler, "Long-time quantum simulation of the primary charge separation in bacterial photosynthesis," *Proceedings of the National Academy of Sciences* **93**, 3926–3931 (1996).
- ²⁴A. Strathearn, P. Kirton, D. Kilda, J. Keeling, and B. W. Lovett, "Efficient non-Markovian quantum dynamics using time-evolving matrix product operators," *Nature Communications* **9**, 3322 (2018).
- ²⁵A. Bose, "Pairwise connected tensor network representation of path integrals," *Physical Review B* **105**, 024309 (2022).
- ²⁶A. Bose and P. L. Walters, "A multisite decomposition of the tensor network path integrals," *The Journal of Chemical Physics* **156**, 024101 (2022).
- ²⁷A. Bose, "Quantum correlation functions through tensor network path integral," *The Journal of Chemical Physics* **159**, 214110 (2023).
- ²⁸A. Bose, "Incorporation of Empirical Gain and Loss Mechanisms in Open Quantum Systems through Path Integral Lindblad Dynamics," *The Journal of Physical Chemistry Letters* **15**, 3363–3368 (2024).
- ²⁹D. Sharma and A. Bose, "Impact of Loss Mechanisms on Linear Spectra of Excitonic and Polaritonic Aggregates," *Journal of Chemical Theory and Computation* **20**, 9522–9532 (2024).
- ³⁰T. Palm and P. Nalbach, "Nonperturbative environmental influence on dephasing," *Physical Review A* **96**, 032105 (2017).
- ³¹A. Bose and P. L. Walters, "Impact of Solvent on State-to-State Population Transport in Multistate Systems Using Coherences," *Journal of Chemical Theory and Computation* **19**, 4828–4836 (2023).
- ³²N. Makri, "The Linear Response Approximation and Its Lowest Order Corrections: An Influence Functional Approach," *The Journal of Physical Chemistry B* **103**, 2823–2829 (1999).
- ³³A. Bose, "Zero-cost corrections to influence functional coefficients from bath response functions," *The Journal of Chemical Physics* **157**, 054107 (2022).
- ³⁴R. P. Feynman and F. L. Vernon, "The theory of a general quantum system interacting with a linear dissipative system," *Annals of Physics* **24**, 118–173 (1963).
- ³⁵A. Bose, "QuantumDynamics.jl: A modular approach to simulations of dynamics of open quantum systems," *The Journal of Chemical Physics* **158**, 204113 (2023).
- ³⁶S. Tretiak, C. Middleton, V. Chernyak, and S. Mukamel, "Bacteriochlorophyll and Carotenoid Excitonic Couplings in the LH2 System of Purple Bacteria," *The Journal of Physical Chemistry B* **104**, 9540–9553 (2000).
- ³⁷A. Freiberg, M. Rätsep, K. Timpmann, and G. Trinkunas, "Excitonic polarons in quasi-one-dimensional LH1 and LH2 bacteriochlorophyll a antenna aggregates from photosynthetic bacteria: A wavelength-dependent selective spectroscopy study," *Chemical Physics* **357**, 102–112 (2009).
- ³⁸A. Bose and N. Makri, "All-Mode Quantum-Classical Path Integral Simulation of Bacteriochlorophyll Dimer Exciton-Vibration Dynamics," *The Journal of Physical Chemistry B* **124**, 5028–5038 (2020).
- ³⁹A. Bose and P. L. Walters, "Impact of Spatial Inhomogeneity on Excitation Energy Transport in the Fenna–Matthews–Olson Complex," *The Journal of Physical Chemistry B* **127**, 7663–7673 (2023).
- ⁴⁰J. del Pino, F. A. Y. N. Schröder, A. W. Chin, J. Feist, and F. J. Garcia-Vidal, "Tensor Network Simulation of Non-Markovian Dynamics in Organic Polaritons," *Physical Review Letters* **121**, 227401 (2018).
- ⁴¹A. Bose and N. Makri, "Non-equilibrium reactive flux: A unified framework for slow and fast reaction kinetics," *The Journal of Chemical Physics* **147**, 152723 (2017).